

## RESEARCH ARTICLE

# Proteomic analysis of the effect of high-fat-diet and voluntary physical activity on mouse liver

Byunghun So<sup>1</sup>, Li Li Ji<sup>2</sup>, Saba Imdad<sup>1,3</sup>, Chounghun Kang<sup>1,4\*</sup>

**1** Molecular Metabolism in Health & Disease, Exercise Physiology Laboratory, Inha University, Incheon, Republic of Korea, **2** Laboratory of Physiological Hygiene and Exercise Science, School of Kinesiology, University of Minnesota Twin Cities, Minneapolis, MN, United States of America, **3** Department of Biomedical Laboratory Science, College of Health Science, Cheongju University, Cheongju, Republic of Korea, **4** Department of Physical Education, College of Education, Inha University, Incheon, Republic of Korea

\* [ck@inha.ac.kr](mailto:ck@inha.ac.kr)**OPEN ACCESS**

**Citation:** So B, Ji LL, Imdad S, Kang C (2022) Proteomic analysis of the effect of high-fat-diet and voluntary physical activity on mouse liver. PLoS ONE 17(8): e0273049. <https://doi.org/10.1371/journal.pone.0273049>

**Editor:** Marcia B. Aguilu, Universidade do Estado do Rio de Janeiro, BRAZIL

**Received:** January 29, 2022

**Accepted:** August 1, 2022

**Published:** August 18, 2022

**Copyright:** © 2022 So et al. This is an open access article distributed under the terms of the [Creative Commons Attribution License](https://creativecommons.org/licenses/by/4.0/), which permits unrestricted use, distribution, and reproduction in any medium, provided the original author and source are credited.

**Data Availability Statement:** All relevant data are within the paper and its [Supporting Information files](#).

**Funding:** This work was supported by INHA UNIVERSITY Research Grant. The funders had no role in study design, data collection and analysis, decision to publish, or preparation of the manuscript.

**Competing interests:** The authors have declared that no competing interests exist.

## Abstract

Nonalcoholic fatty liver disease (NAFLD), characterized by an abnormal accumulation of triglycerides in hepatocytes, is closely linked to insulin resistance, metabolic syndrome, and changes in lipogenesis in the liver. The accumulation of hepatic lipids can lead to a range of pathologies from mild steatosis to severe cirrhosis. Endurance exercise is known to ameliorate the adverse health effects of NAFLD. Therefore, we aimed to investigate the effect of voluntary wheel running (VWR) on the metabolic changes in the livers of high-fat diet (HFD)-induced NAFLD mice and used LC-MS/MS (Liquid chromatography–mass spectrometry) to determine whether the tested intervention affected the protein expression profiles of the mouse livers. Male C57BL/6 mice were randomly divided into three groups: control (CON), high-fat diet sedentary group (HFD), high-fat diet VWR group (HFX). HFX group performed voluntary wheel running into individually cages, given a high-fat diet for 12 weeks. Food consumption, body weight, and running distance were measured every week. Using 2D (2-dimensional)-gel electrophoresis, we detected and quantitatively analyzed the protein expression with >2.0-fold change in the livers of HFD-fed mice, HFD-fed exercise (HFX) mice, and chow-fed mice. Body weight was significantly increased in HFD compared to CON ( $P < 0.05$ ). The 2D-gel electrophoresis analysis indicated that there was a difference between CON and HFD groups, showing 31 increased and 27 decreased spots in the total 302 paired spots in the HFD group compared to CON. The analysis showed 43 increased and 17 decreased spots in the total 258 spots in the HFX group compared to CON. Moreover, 12 weeks of VWR showed an increase of 35 and a decrease of 8 spots in a total of 264 paired spots between HFD and HFX. LC-MS/MS of HFD group revealed that proteins involved in ketogenesis, lipid metabolism, and the metabolism of drugs and xenobiotics were upregulated, whereas detoxifying proteins, mitochondrial precursors, transport proteins, proteasomes, and proteins involved in amino acid metabolism were downregulated. On the other hand, VWR counteracted the protein expression profile of HFD-fed mice by upregulating molecular chaperones, gluconeogenesis-, detoxification-, proteasome-, and energy metabolism-related proteins. This study provided a molecular understanding of the

HFD- and exercise-induced protein marker expression and presented the beneficial effects of exercise during pathophysiological conditions.

## Introduction

Nonalcoholic fatty liver disease (NAFLD) is a condition in which excessive triglyceride (TG) accumulation in hepatocytes results in steatosis and inflammation [1, 2]. The pathophysiology of NAFLD ranges from nonalcoholic steatohepatitis, which increases the inflammatory response and hepatocyte fibrosis to hepatic cirrhosis and hepatocellular carcinoma [3, 4]. A growing number of studies suggest that NAFLD is associated with metabolic syndrome-related diseases [5], such as type 2 diabetes, obesity, and dyslipidemia, and significantly increases the risk of cardiovascular disease [6]. Excessive caloric intake, including a high-fat diet (HFD) and inactivity, plays a critical role in the development of NAFLD [7]. In addition, HFD-induced metabolic disorders are intimately linked to and promoted by high availability of plasma free fatty acids in the liver [8].

Above all, early NAFLD treatment is essential to prevent severe liver disease, but so far, there is no approved medication available for NAFLD. However, numerous studies have attempted to explore and find an effective solution to attenuate NAFLD development, including calorie restriction and physical exercise [9–11]. Regular exercise is an effective regimen for the prevention and treatment of metabolic disorders. The principal advantage of exercise in NAFLD is improved insulin sensitivity and lipid profile, and a reduction in the fat accumulation in the liver [11].

Several studies have been conducted to investigate the beneficial effects of exercise using HFD models. A comparison of the effects of forced treadmill and voluntary wheel running exercise in a mouse model showed a similar change of physiologic effects, such as weight, fat mass, and mitochondrial biogenesis markers [12]. However, it is commonly known that forced treadmill exercise can be adjusted in duration and intensity, while VWR can help to become habitual with continued access to participate in aerobic exercise [13]. Forced treadmill exercise was demonstrated to enhance fatty acid oxidation by improving mitochondrial function and suppressing lipogenesis expression in the liver [14, 15]. In addition, endurance exercise was reported to ameliorate HFD-induced mitochondrial function in the liver, such as that related to the mitochondrial transmembrane electric potential and fat oxidation [16]. Several studies showed that VWR can protect against inflammatory markers in adipose tissue and ameliorate insulin sensitivity in diet-induced obese mouse model [17–19]. Ghareghani et al. demonstrated that aerobic endurance training can reduce lipogenesis by miR-33-mediated autophagy, which regulates cholesterol homeostasis in an HFD model [20]. To date, despite the accumulating evidence of the positive effects of exercise in the HFD model, studies to find exercise-related protein marker profile are needed for further research.

High-throughput techniques can fill the knowledge gap regarding the elucidation of the underlying mechanism of exercise intervention in metabolic disorders at the level of individual genes or translational proteins [21, 22]. Several studies have suggested that proteomics is a powerful tool for assessing quantitative protein expression in specific organs [22, 23]. Previous studies have demonstrated the impact of HFD on mouse liver gene expression to quantitatively screen and identify protein expression patterns using MS/MS analysis [24, 25].

In the present study, we investigated the protein expression profiles in the liver of HFD-fed mice under sedentary and aerobic exercise conditions to understand the underlying molecular

mechanisms associated with the protective effects of exercise. We screened for proteins involved in *de novo* synthesis, energy metabolism, and mitochondrial function in the HFD mouse model using LC-MS/MS.

## Materials and methods

### Experimental animals and sample preparation

Five-week-old mice (30 male, C57BL/6, DBL Co., Korea) were purchased and randomly assigned to three groups: CON, control group (n = 9); HFD, high-fat diet sedentary group (n = 9); HFX, high-fat diet VWR group (n = 12). The CON group was fed a chow diet (18% protein, 5% fat, 5% fiber, 5% ash, RodFeed, DBL, Co., Korea) and the HFD group was fed a high-fat diet (34.9% fat by weight, providing 60% calories from fat, D12492, Research diets, Co., USA) for 12 weeks. The animals were maintained in a room with constant temperature of  $22 \pm 1^\circ\text{C}$  and humidity-controlled environment  $55 \pm 10\%$  with a 12-light/12-h dark cycle and free access to food and water. Body weight and food intake of the animals were measured weekly. The institutional animal care and use committee of Chungbuk National University reviewed and approved the study design before the animal experiments were conducted (CBNUA-1214-18-01). The procedures for the handling and care of the animals adhered to the guidelines that comply with the current international laws and policies (NIH Guide for the Care and Use of Laboratory Animals, NIH Publication No. 85–23, 1985, revised 1996) [26]. All experiments were conducted to minimize the number of animals used and the possible suffering/pain that may be caused by any of the experimental procedures used in the present study.

The mice were anesthetized with 2.5% flow rate of isoflurane (Sigma-Aldrich, USA) using Multiplus-MEVD anesthesia machine with ventilator (Royal Medical Co., Korea), and were sacrificed immediately post anesthesia by cervical dislocation. Frozen liver tissues (200 mg) were solubilized in 1.0 ml of lysis buffer consisting of 7 M urea, 2M thiourea, 4% w/v CHAPS, 100 mM dithiolerythritol DTE, 40 mM Tris, 2% v/v pH 3–10 Bio-Lytes (Bio-rad, Hercules, CA, USA) and a trace of bromphenole blue. Solubilization was aided by tip-probe sonication for 4 x 30s with 2min on ice between each round of sonication. Samples were centrifuged at 12000 g at  $4^\circ\text{C}$  for 1 h. The supernatant was transferred into new tubes, and then 150 U of endonuclease (Sigma, St. Louis, MO, USA) was added. Protein samples were stored at  $-80^\circ\text{C}$  until use.

### Voluntary wheel running

The HFX group was individually housed, and a running wheel (Lafayette Instrument Company, USA) was placed in each cage for 12 weeks. Running activities such as distance (meter) and velocity (meter per minute) were recorded in a 10-min time interval using a computerized system (Lafayette instrument computerized animal wheel monitoring system; Lafayette Instrument Co., USA).

### 2D-Polyacrylamide gel electrophoresis

2D-Polyacrylamide gel electrophoresis (PAGE) was performed as described previously [27, 28]. Aliquots in sample buffer (7 M urea, 2M thiourea, 4.5% CHAPS, 100 mM DTE, 40 mM Tris, pH 8.8) were applied to the immobilized non-linear gradient (pH 3–10) strips (Amersham Biosciences, Uppsala, Sweden). Isoelectric focusing was performed at 80,000 Vh (volt-hour). The second dimension was analyzed on 9%–16% linear gradient polyacrylamide gels (18 cm × 20 cm × 1.5 mm) at a constant 40 mA per gel for approximately 5 h. After protein fixation in 40% methanol and 5% phosphoric acid for 1 h, the gels were stained with Coomassie

Brilliant Blue G-250 for 12 h. The gels were then destained with H<sub>2</sub>O, scanned in a Bio-Rad (Richmond, CA) GS710 densitometer, and converted into electronic files, which were then analyzed with Image Master Platinum 5.0 (Amersham Biosciences).

### LC-MS/MS for peptide analysis

Nano LC-MS/MS analysis was performed with an Easy n-LC (Thermo Fisher San Jose, CA, USA) and an LTQ Orbitrap XL mass spectrometer (Thermo Fisher, San Jose, CA, USA) equipped with a nano-electrospray source. Samples were separated on a C18 nanopore column (150 mm × 0.1 mm, 3 μm pore size; Agilent). Mobile phase A for LC separation was 0.1% formic acid and 3% acetonitrile in deionized water, and mobile phase B was 0.1% formic acid in acetonitrile [28]. The chromatography gradient was designed for a linear increase from 0% B to 60% B in 9 min, 60% B to 90% B in 1 min, and 3% B in 5 min. The flow rate was maintained at 1800 nL/min.

Mass spectra were acquired using data-dependent acquisition with a full mass scan (380–1700 *m/z*) followed by 10 MS/MS scans. For MS1 full scans, the orbitrap resolution was 15,000, and the automatic gain control (AGC) was  $2 \times 10^5$ . For MS/MS in the LTQ, the AGC was  $1 \times 10^4$ .

### Database search

The mascot algorithm (Matrixscience, USA) was used to identify peptide sequences present in a protein sequence database. Database search criteria were taxonomy: *Mus musculus*, fixed modification; carbamidomethylated at cysteine residues; variable modification; oxidized at methionine residues, maximum allowed missed cleavage, 2; MS tolerance, 10 ppm; MS/MS tolerance, 0.8 Da. The peptides were filtered using a significance threshold of  $P < 0.05$ .

### Statistical and network analysis

Experimental data were expressed as mean ± standard error of the mean (SEM), and the effect of time and exercise on physiological parameters such as weight and food intake were analyzed using two-way ANOVA with Tukey-Kramer post-hoc test with a standard significance threshold ( $P < 0.05$ ). GraphPad Prism 8.0 (CA, USA) was used for statistical analysis. To analyze the interactions between HFD-dysregulated proteins and HFX-upregulated proteins found in this study, we uploaded differentially regulated metabolism-related proteins, with a significance of >2.0-fold, to the STRING database (Search Tool for the Retrieval of Interacting Genes/Proteins, version 11.0) to search for protein–protein interactions.

## Results

### Impact of VWR on body weight and food uptake

[Fig 1A](#) demonstrate the weekly body weight for each group. HFD induced a significant weight gain from 3-week to 12-week period in the HFD group compared to the CON group ( $P < 0.001$ ). High fat diet had a very significant effect on the body weights [ $F(22, 324) = 12.88$ ,  $P < 0.001$ ]. However, voluntary wheel running for 12 weeks prevented weight gain in the HFX group ( $P < 0.001$ ). The food intake was higher in the CON group than in the HFD group [ $F(22, 324) = 3.844$ ,  $P < 0.001$ ; [Fig 1B](#)]. In contrast, there was no difference in the food consumption between the HFD and HFX groups after 12 weeks. When the body weights of the mice were normalized, we found that the food intake of mice was significantly higher in the CON group than the other groups. And HFX group had a higher food intake than HFD group ( $P < 0.001$ , [Fig 1C](#)). Moreover, cumulative food intake was significantly higher in the CON

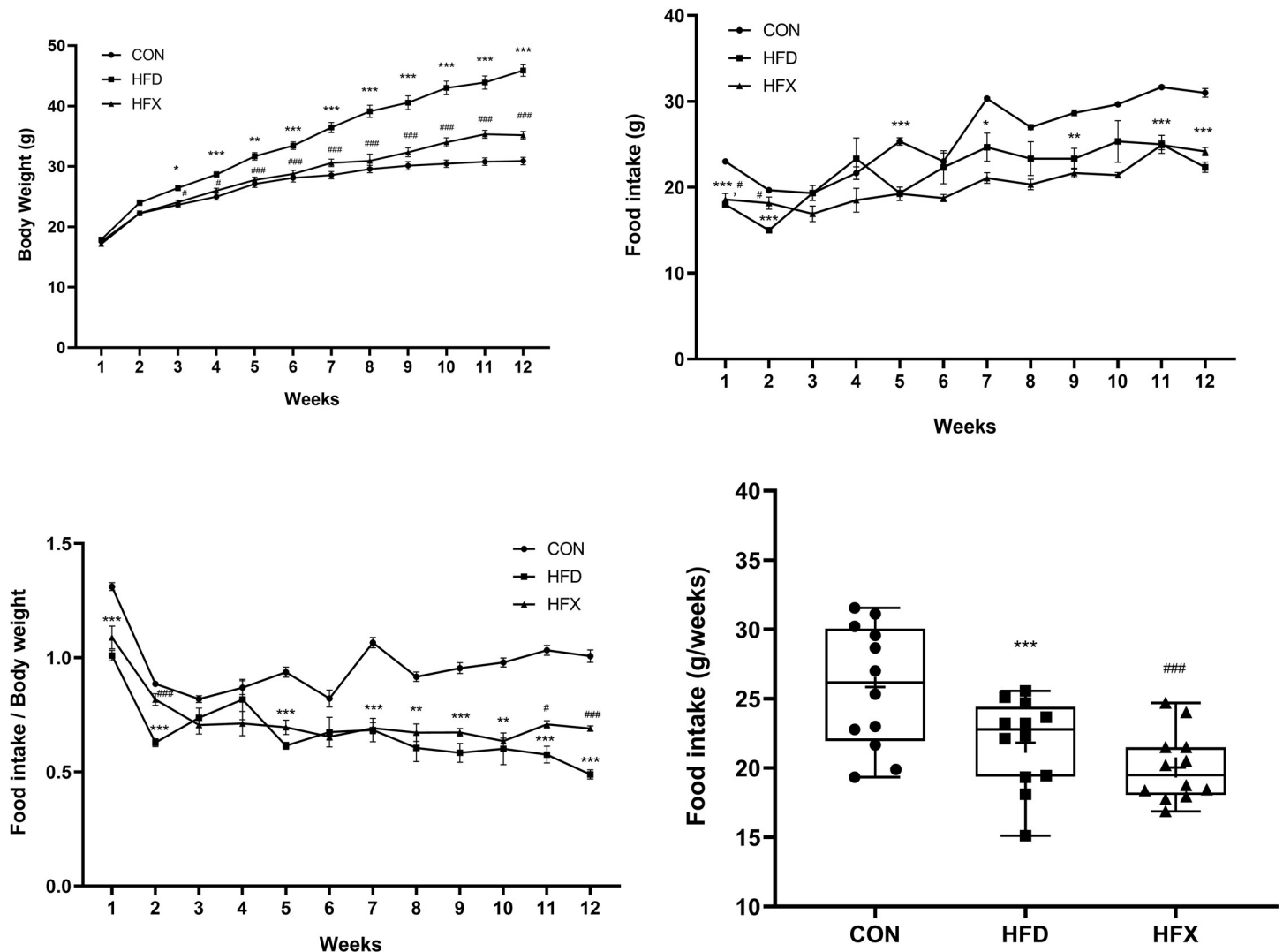


**Fig 1. The effects of a high-fat diet and voluntary wheel running (VWR) on body weight, food intake.** C57BL/6 mice were fed a high-fat diet (HFD), a high-fat fed with VWR (HFX), and corresponding control diet (CON) for 12 weeks. (A) The body weight curve of the CON, HFD, and HFX group was monitored. (B) Weekly food intake of the CON, HFD, and HFX group for 12 weeks. (C) The ratio of weekly average food intake to body weight for all experimental groups. (D) Distribution of food intake for all experimental groups. The data represent means  $\pm$  SEM of (A-D)  $n = 9$ , the control group (CON);  $n = 9$ , the high-fat diet group (HFD);  $n = 12$ , the high-fat diet VWR group (HFX). \*\* $P < 0.01$ , \*\*\* $P < 0.001$  compared with CON and ## $P < 0.01$ , ### $P < 0.001$  compared with HFD, using two-way ANOVA with Tukey-Kramer post-hoc test with a standard significance threshold ( $P < 0.05$ ) (A-D).

<https://doi.org/10.1371/journal.pone.0273049.g001>

group than HFD group ( $P < 0.001$ ), while the HFX group had a decreased cumulative intake as compared to HFD group ( $P < 0.001$ , Fig 1D). In addition, VWR showed a gradual decrease in the running distance over time in the HFX group, at the individual level and a large variation was observed in the total running distance ranging from about 113 km to 247 km in the HFX group (S1 Fig).

## 2D-PAGE analysis

2D-PAGE analysis of the mouse liver showed a total of 393 and 358 protein spots for the CON and HFD groups, respectively, with 147 non-paired spots between the two groups. There were 302 paired protein spots between the CON and HFD groups, which were used for further

analysis. Among the 302 paired spots, 31 protein spots were found to be upregulated, while 27 spots were downregulated in the HFD group compared with the CON group (Fig 2A–2D).

Among the total 343 protein spots detected in the HFX group, 268 were paired spots between CON and HFX, while the number of non-paired spots was 200. Analysis of the 268 paired spots revealed 43 upregulated and 17 downregulated proteins in the HFX group (Fig 3A–3D). Among the 264 paired spots found between the HFD and HFX groups, 35 protein spots corresponded with upregulated, while 8 spots corresponded with downregulated proteins in the HFX group. A total of 173 non-paired protein spots were detected (Fig 4A–4D). The differentially expressed proteins showed a difference of >2.0-fold.

### Proteomic analysis of mouse liver

The proteomic analysis of the mouse livers using 2D-PAGE followed by protein identification by LC-MS/MS revealed 35 protein spots whose expression levels were changed by > 2.0-fold with significant alterations ( $P < 0.05$ ) in the HFD vs. CON (Table 1), HFX vs. CON groups (Table 2) and the HFX vs. HFD groups (Table 3). According to their functional properties, the identified proteins were grouped into the following nine categories:

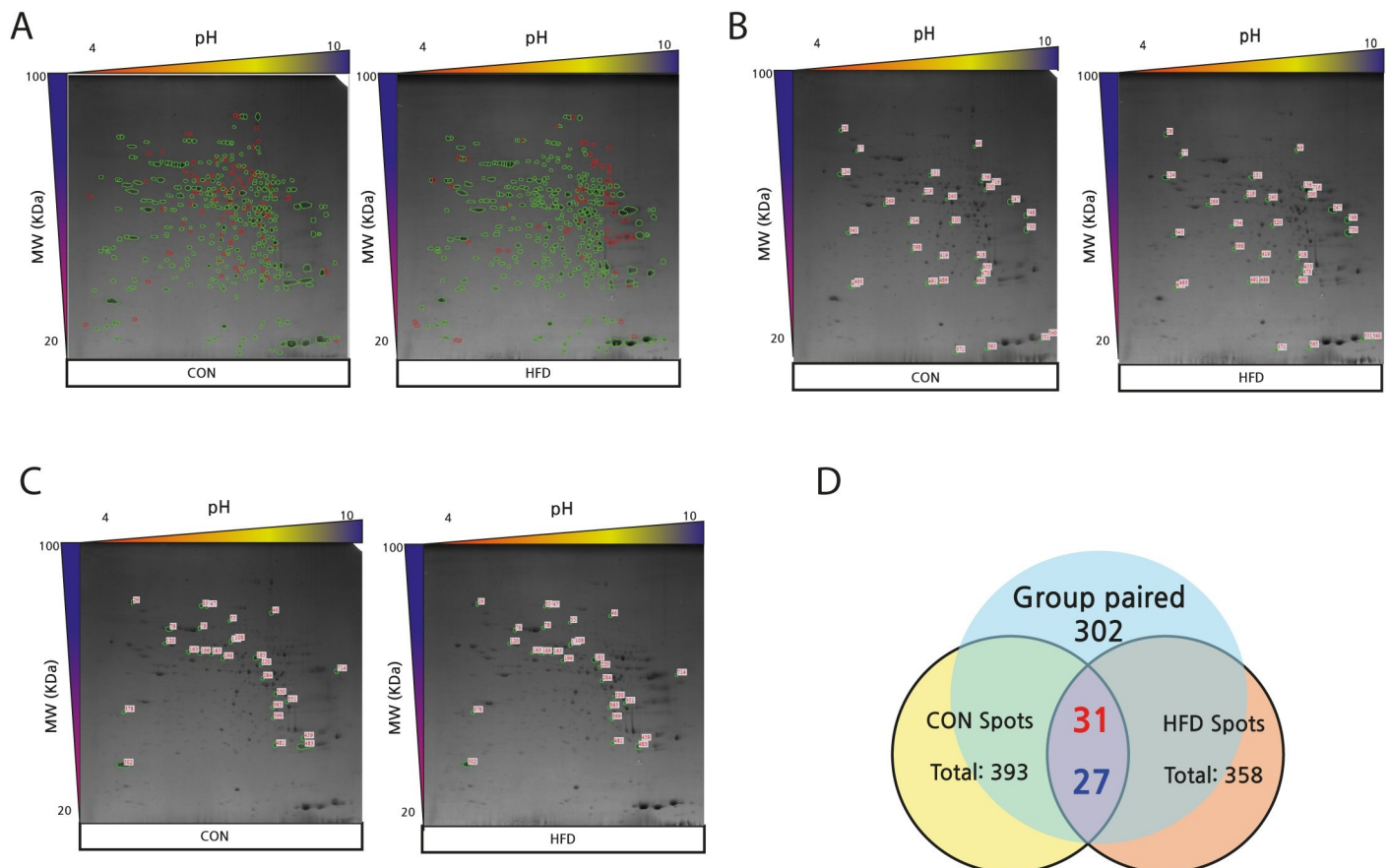


**Fig 2.** 2D-PAGE images and Venn diagram showing differential protein expression (>2-fold) between CON and HFD groups (A–D). (A) The images of 2D-PAGE show green circles indicating group paired spots, and red circles indicating group non-paired spots. Green circles indicate group paired spots, and orange circles indicate group non-paired spots. The images of the 2D-PAGE show an increase of 31 spots (B) and a decrease of 27 spots (C) among the 302 paired spots in HFD compared to CON. The differentially expressed spots showed a difference of >2.0-fold. (D) The numbers in red denote upregulated spots and the numbers in blue indicate downregulated spots, in the Venn diagram.

<https://doi.org/10.1371/journal.pone.0273049.g002>

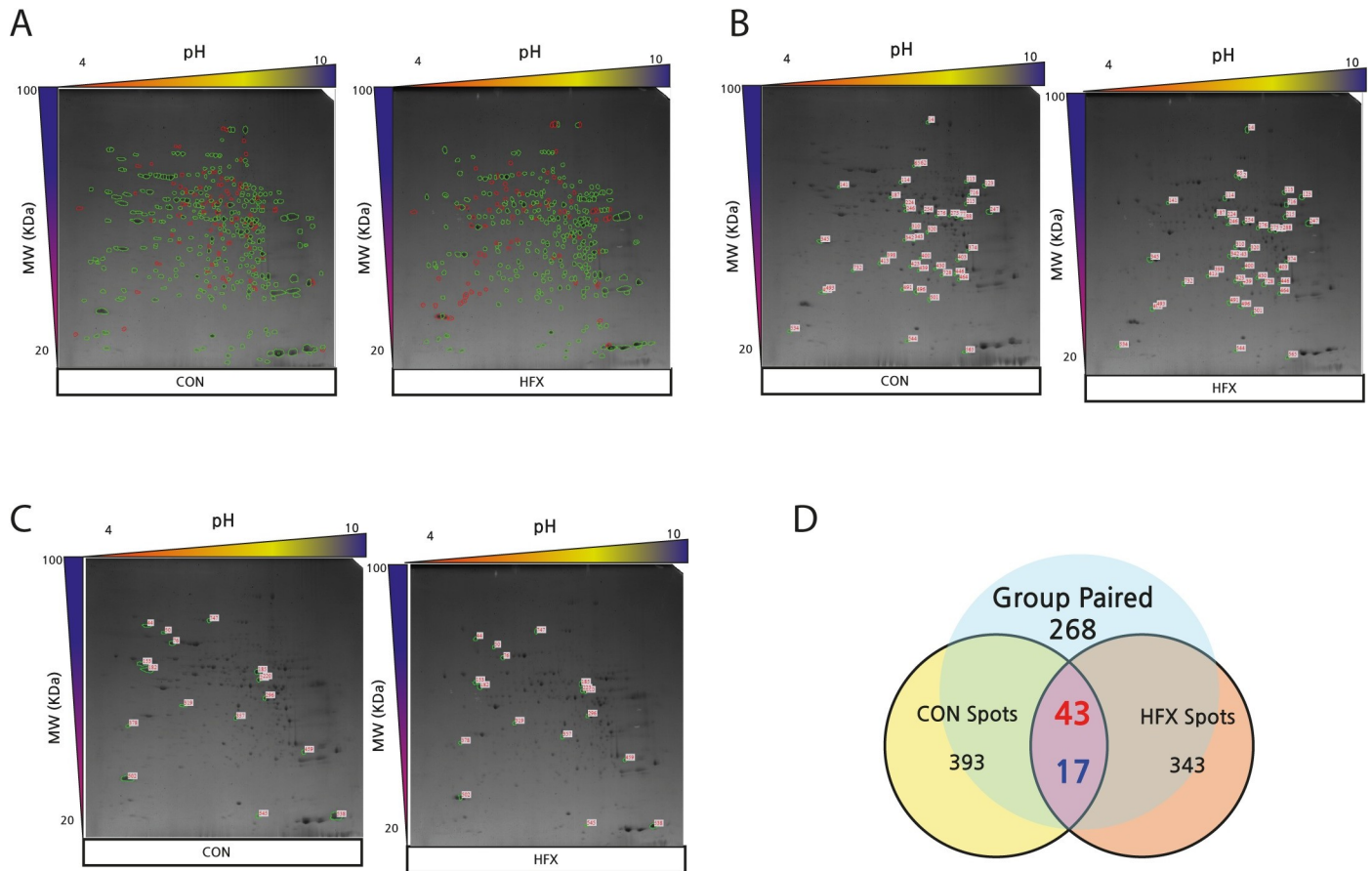


**Fig 3. 2D-PAGE images and Venn diagram showing differential protein expression (>2-fold) between CON and HFX (A-D).** (A) The images of 2D-PAGE show green circles which indicate group paired spots, and red circles that indicate group non-paired spots. Green circles indicate group paired spots, and orange circles indicate group non-paired spots. The images of the 2D-PAGE show an increase of 43 spots (B) and a decrease of 17 spots (C) among the 268 paired spots in HFD compared to CON. The differentially expressed spots showed a difference of >2.0-fold. (D) The numbers in red denote upregulated spots and the numbers in blue indicate downregulated spots, in the Venn diagram.

<https://doi.org/10.1371/journal.pone.0273049.g003>

1. Proteins involved in carbohydrate, lipid, and energy metabolism, such as fructose-1,6-bisphosphate 1 (Fbp1), ATP synthase (mt-Atp8), ATP5b protein (Atp5b), and enolase 1 B (Eno1b)
2. Proteins involved in amino acid metabolism, such as phenylalanine hydroxylase (Pah), isovaleryl-CoA dehydrogenase (Ivd), and carboxylesterase 3 B (Ces3b)
3. Mitochondrial precursors, such as isovaleryl-CoA dehydrogenase (Ivd), cytochrome b-c1 complex subunit 2 (Uqcrc2), 3-hydroxy-3-methylglutaryl-coenzyme synthase 2 (Hmgcs2), 3-hydroxy-3-methylglutaryl-CoA synthase (Hmgcs2), and 3-hydroxy-3-methylglutaryl-CoA lyase (Hmgcl1)
4. Molecular chaperones, such as heat shock protein 90-beta membrane 1 (Fkbp4)
5. Proteins involved in detoxification, such as glutathione S-transferases (Gstp1) and glutathione peroxidase 6 (Gpx6), the crystal structure of a murine alpha-class glutathione S-transferase (1GUK\_A)
6. Protein transporters, such as selenium-binding protein (Selenbp2)

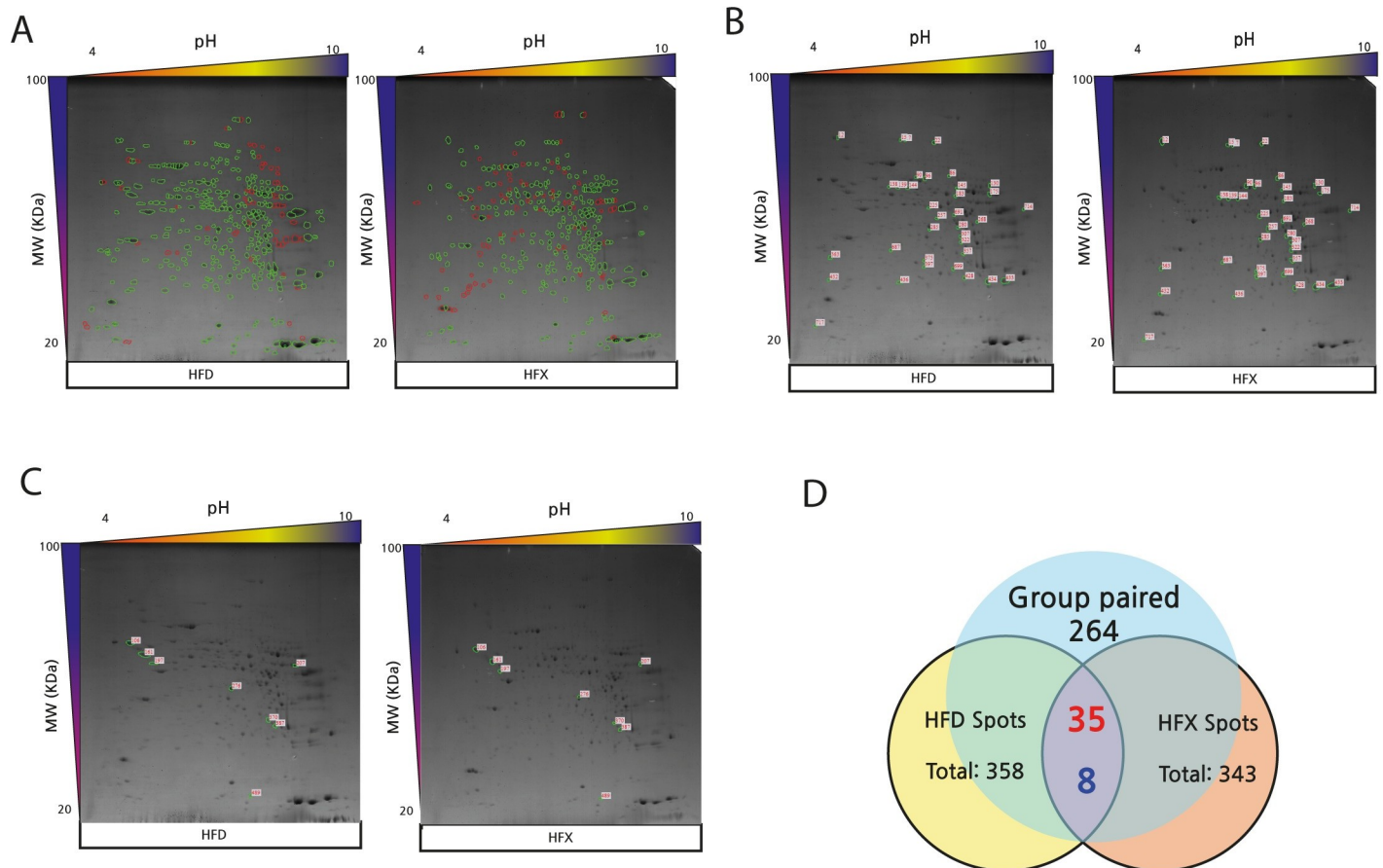


**Fig 4. 2D-PAGE images and Venn diagram showing differential protein expression (>2-fold) between HFD and HFX (A-D).** (A) The images of 2D-PAGE show green circles that indicate group paired spots, and red circles that indicate group non-paired spots. Green circles indicate group paired spots, and orange circles indicate group non-paired spots. The images of the 2D-PAGE show an increase of 35 spots (B) and a decrease of 8 spots (C) among the 264 paired spots in HFD compared to CON. The differentially expressed spots showed a difference of >2.0-fold. (D) The numbers in red denote upregulated spots and the numbers in blue indicate downregulated spots, in the Venn diagram.

<https://doi.org/10.1371/journal.pone.0273049.g004>

7. Proteolysis proteins, such as proteasome activator subunit 4 (Psme4)
8. Enzymes, such as Aldh1l1 (Aldh1l1)
9. Unknown functional proteins, such as the mCG8752 isoform CRA\_c, mCG8752 isoform CRA\_b, and mCG129115 (Fig 5).

### Impact of HFD on biochemical pathways

To determine a functional network or interaction between the HFD and HFX protein regulation profiles, we performed four functional association analyses using the STRING database (version 11.0, <https://string-db.org>) on 35 protein spots. The network showed that database (light blue lines) and co-expression (black lines) associations are generated from a list of significant protein interaction groups gathered from curated databases. The experimental association (pink lines) was extracted from a list of significant protein interaction datasets gathered from other protein-protein interaction databases, such as IMEx and MIntAct. The text mining associations (light green lines) were extracted from published scientific literature. The majority of these 28 differentially regulated proteins showed protein-protein interactions (PPI) in all



Table 1. Liver proteins differentially expressed in the HFD vs. CON.

Accession Number	Symbols	Protein name	Mass	Total Mascot score	Matched peptide	Sequences	Calculated PI	Sequence Coverage	emPAI	Fold change (HFD/CON)	Spot number
AAH48380.1	Ces3b	Carboxylesterase 3B	63790	52	1(1)	1(1)	5.79	1	0.11	1.2	114
NP_062287.1	Selenbp2	selenium-binding protein 2	53165	933	97(97)	15(15)	5.78	31	3.13	-3.4	165
NP_062287.1	Selenbp2	selenium-binding protein 2	53165	1075	90(90)	18(18)	5.78	31	4.92	-2.5	166
NP_058054.2	Hmgcs2	ATP synthase subunit beta	56265	1464	253(253)	19(19)	5.19	40	8.62	1.1	182
AAH37127.1	Atp5b	Atp5b protein	56632	597	28(28)	10(10)	5.24	23	1.73	-1.2	215
EDL38956.1	Hmgcs2	3-hydroxy-3-methylglutaryl-Coenzyme A synthase 2	59142	509	13(13)	9(9)	8.36	14	1.10	1.9	217
EDL21456.1	Pah	phenylalanine hydroxylase	50265	506	22(22)	11(11)	5.91	20	1.84	1.2	224
NP_001020559.1	Eno1b	enolase 1B	47453	1129	51(51)	20(20)	6.37	31	7.87	-1.4	254
NP_062800.1	Ivd	isovaleryl-CoA dehydrogenase	44695	626	30(30)	11(11)	8.53	23	3.56	-2.2	284
AAB03107.1	Hmgcll1	3-hydroxy-3-methylglutaryl-CoA lyase	34641	44	1(1)	1(1)	8.70	2	0.15	-2.9	365
EDL26822.1	Psme4	proteasome	31081	139	2(2)	2(2)	8.80	6	0.37	-1.3	423
EDL01226.1	mCG8752	mCG8752, isoform CRA_b	31728	262	10(10)	5(5)	6.47	15	1.10	-2.1	399
NP_038569.1	Gstp1	glutathione S-transferase P 1	23765	209	4(4)	3(3)	7.68	18	1.20	-3.9	483
1GUK_A	1GUK_A	Chain A, Crystal Structure of Murine Alpha-Class Gsta4-4	25559	534	23(23)	11(11)	6.77	38	6.54	-3.7	481
EDL31590.1	mt-Atp8	ATP synthase	17589	158	6(6)	2(2)	5.01	16	0.70	-1.3	534

<https://doi.org/10.1371/journal.pone.0273049.t001>

four association algorithms. In the protein network, mt-Atp8, Uqcrc2, and Atp5b, which were related to electron transport chain (ETC), exhibited more interactions than the other proteins. Interestingly, those three proteins mentioned above were also downregulated in the HFD but were upregulated by the physical activity in the HFX group (Fig 6).

## Discussion

High-fat diet induces the development of NAFLD, the most widespread chronic liver disease in many regions of the globe, especially in Western countries [29, 30]. NAFLD is also considered an independent predictor of cardiovascular diseases and increases the risk of chronic kidney disease [31]. However, the current therapeutic outcomes for dealing with NAFLD-related metabolic pathologies are unsatisfactory [32]. In line with this, exercise has been proposed as an effective treatment strategy for NAFLD through various mechanisms, such as the upregulation of antioxidant enzymes and anti-inflammatory mediators and through the regulation of the endoplasmic reticulum stress-associated pathways [33, 34]. In light of these studies, we identified the HFD-induced NAFLD-linked protein expression profile in sedentary and exercise intervention mouse models through a high-throughput quantification of proteins.

Firstly, we found a significantly increased body weight in HFD group ( $P < 0.001$ , Fig 1A), but VWR prevented the weight gain in HFX group ( $P < 0.001$ ). The food intake was decreased

Table 2. Liver proteins differentially expressed in the HFX vs. CON.

Accession Number	Symbols	Protein name	Mass	Total Mascot score	Matched peptide	Sequences	Calculated PI	Sequence Coverage	emPAI	Fold change (HFX/CON)	Spot number
AAH48380.1	Ces3b	Carboxylesterase 3B	63790	52	1(1)	1(1)	5.79	1	0.11	4.2	114
NP_062287.1	Selenbp2	selenium-binding protein 2	53165	933	97(97)	15(15)	5.78	31	3.13	1.1	165
NP_062287.1	Selenbp2	selenium-binding protein 2	53165	1075	90(90)	18(18)	5.78	31	4.92	1.2	166
NP_058054.2	Hmgcs2	ATP synthase subunit beta	56265	1464	253(253)	19(19)	5.19	40	8.62	-2.1	182
AAH37127.1	Atp5b	Atp5b protein	56632	597	28(28)	10(10)	5.24	23	1.73	2.6	215
EDL38956.1	Hmgcs2	3-hydroxy-3-methylglutaryl-Coenzyme A synthase 2	59142	509	13(13)	9(9)	8.36	14	1.10	-1.9	217
EDL21456.1	Pah	phenylalanine hydroxylase	50265	506	22(22)	11(11)	5.91	20	1.84	4.9	224
NP_001020559.1	Eno1b	enolase 1B	47453	1129	51(51)	20(20)	6.37	31	7.87	2.7	254
NP_062800.1	Ivd	isovaleryl-CoA dehydrogenase	44695	626	30(30)	11(11)	8.53	23	3.56	1.1	284
AAB03107.1	Hmgcll1	3-hydroxy-3-methylglutaryl-CoA lyase	34641	44	1(1)	1(1)	8.70	2	0.15	1.6	365
EDL26822.1	Psme4	proteasome	31081	139	2(2)	2(2)	8.80	6	0.37	2.5	423
EDL01226.1	mCG8752	mCG8752, isoform CRA_b	31728	262	10(10)	5(5)	6.47	15	1.10	1.2	399
NP_038569.1	Gstp1	glutathione S-transferase P 1	23765	209	4(4)	3(3)	7.68	18	1.20	-1.8	483
1GUK_A	1GUK_A	Chain A, Crystal Structure of Murine Alpha-Class Gsta4-4	25559	534	23(23)	11(11)	6.77	38	6.54	1.2	481
EDL31590.1	mt-Atp8	ATP synthase	17589	158	6(6)	2(2)	5.01	16	0.70	2.3	534

<https://doi.org/10.1371/journal.pone.0273049.t002>

over time in HFD group ( $P < 0.001$ ), but the normalization of the body weights yielded a significantly increased food intake in HFX group ( $P < 0.001$ ). In addition, the cumulative food intake of mice was significantly different among groups over time ( $P < 0.001$ , Fig 1D). Our results were supported by a recent study which demonstrated that VWR (for 30 min, 5 days) reduces weight gain by preferentially decreasing the intake of high-fat food [35]. Our data showed that HFX group consumed the lowest cumulative food intake among all groups, corroborating with the aforementioned report.

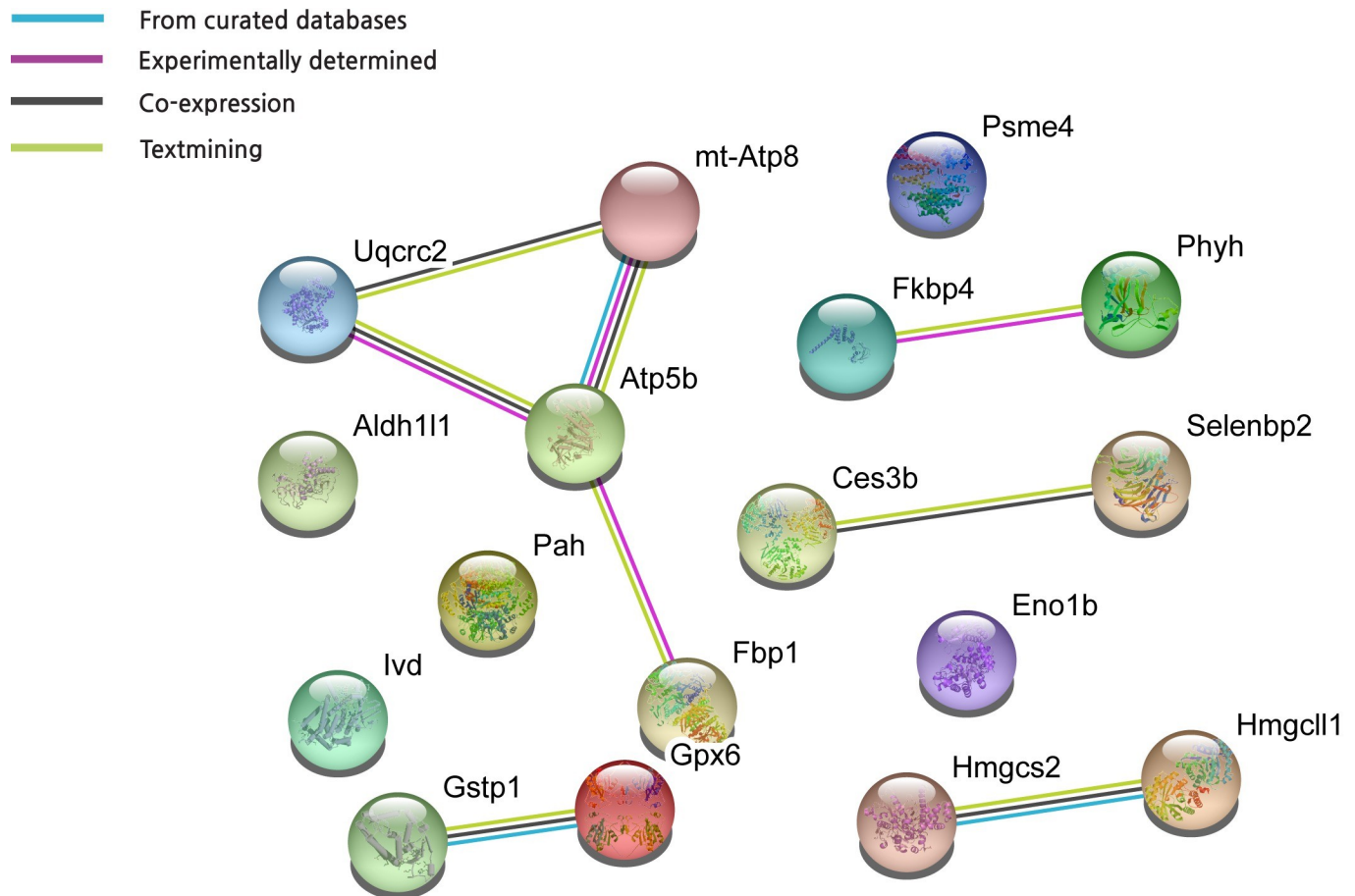
Next, we analyzed the quantitative protein expression profile among groups and established that the level of enolase 1B was higher in the HFD group than in the CON group. Enolase is a glycolytic enzyme which plays an important role of catalyzing 2-phosphoglycerate dehydration to phosphoenolpyruvate as part of glycolytic and gluconeogenesis pathway [36]. Enolase 1 (enolase alpha) is known as a diagnostic marker of multiple tumors and numerous autoimmune diseases [37], including rheumatoid arthritis [38]. A recent study demonstrated that enolase1/MBP-1, functions as a tumor suppressor by binding and inhibiting *c-myc* promoter-binding protein and could play the role of an important sensor/regulator in stressful conditions [39, 40]. In addition, upregulation of enolase 3 in human liver cell line could promote the lipid accumulation. The higher levels of enolase 1B in HFD group suggested that 12 weeks of HFD intake might induce an excessive fat accumulation and cause inflammation and damage

Table 3. Liver proteins differentially expressed in the HFX vs. HFD.

Accession Number	Symbols	Protein name	Mass	Total Mascot score	Matched peptide	Sequences	Calculated PI	Sequence Coverage	emPAI	Fold change (HFX/HFD)	Spot number
AAH10445.1	Fkbp4	Hsp90b1 Heat shock protein 90, beta (Grp94), member 1	92717	2808	87(87)	55(55)	4.74	42	21.44	5.7	12
AAH24055.1	Aldh1l1	Aldh1l1 protein	99527	1323	42(42)	26(26)	5.69	25	3.16	3.7	15
AAH48380.1	Ces3b	Carboxylesterase 3B	63790	52	1(1)	1(1)	5.79	1	0.11	4.2	90
NP_062287.1	Selenbp2	selenium-binding protein 2	53165	752	43(43)	12(12)	5.78	23	2.46	3.8	138
NP_062287.1	Selenbp2	selenium-binding protein 2	53165	1432	97(97)	23(23)	5.78	37	9.04	3.2	139
NP_062287.1	Selenbp2	selenium-binding protein 2	53165	1594	127(127)	23(23)	5.78	47	8.55	3.8	144
NP_062287.1	Selenbp2	selenium-binding protein 2	53165	455	18(18)	8(8)	5.78	17	1.03	4.6	145
NP_062287.1	Selenbp2	selenium-binding protein 2	53165	212	5(5)	4(4)	5.78	7	0.43	3.3	183
NP_032282.2	Hmgcs2	hydroxymethylglutaryl-CoA synthase	57300	1115	120(120)	19(19)	8.65	27	4.64	-2.5	207
NP_032282.2	Hmgcs2	hydroxymethylglutaryl-CoA synthase	57300	201	7(7)	4(4)	8.65	7	0.39	2.5	370
EDL01201.1	mCG129115	mCG129115	52628	144	3(3)	3(3)	4.95	5	0.31	-2.9	197
CAA27558.1	Gpx6	glutathione peroxidase	22504	335	10(10)	6(6)	6.74	32	3.28	2.7	225
NP_062800.1	Ivd	isovaleryl-CoA dehydrogenase	46695	933	65(65)	17(17)	8.53	29	7.36	2.5	691
NP_062268.1	Fbp1	fructose-1,6-bisphosphatase 1	37288	1185	97(97)	18(18)	6.15	38	11.47	5.2	285
BAA19003.1	Phyh	LN1	39053	542	23(23)	12(12)	7.64	26	6.97	4.6	322
EDL01227.1	mCG8752	mCG8752, isoform CRA_c	50255	802	59(59)	13(13)	6.02	26	2.72	2.6	357
EDL26822.1	Psme4	proteasome	31081	139	2(2)	2(2)	8.80	6	0.37	2.5	375
NP_038569.1	Gstp1	glutathione S-transferase P 1	23765	345	19(19)	5(5)	7.68	28	4.90	4.4	428
NP_080175.1	Uqcrc2	cytochrome b-c1 complex subunit 2	48262	971	34(34)	16(16)	9.26	30	5.09	3.4	714
EDL31590.1	mt-Atp8	ATP synthase	17589	158	6(6)	2(2)	5.01	16	0.70	2.3	717

<https://doi.org/10.1371/journal.pone.0273049.t003>

to the liver [41]. Our results indicated that the majority of the differentially expressed proteins in the livers of HFD and HFX mice were involved in the energy metabolism of carbohydrates and lipids, as reported previously [42, 43]. Fbp1, a rate-limiting enzyme in gluconeogenesis, is involved in regulating the hydrolysis of fructose 1,6-bisphosphate to fructose 6-phosphate [44, 45]. The accelerated energy expenditure by regular exercise maintains glucose homeostasis in working skeletal muscles through increased glucose uptake and utilization of lipids and muscle glycogen [46]. During prolonged exercise periods such as VWR, the requirement of glucose uptake by contracting muscles is supported by energy homeostasis in the form of glucose release from the liver [47]. Our data demonstrated an increase in liver Fbp1 protein expression after VWR in the HFX group compared with the HFD group. This finding was consistent with previous studies showing that regular exercise could activate metabolic pathways, such as gluconeogenesis, by the oxidation of fatty acids by the liver to fulfill the energy demand. Furthermore, the data suggested that increased gluconeogenesis reflects the increased mitochondrial redox state. Atp5b and mt-Atp8 are mitochondrial membrane ATP synthases that produce ATP from ADP in a proton gradient across the membrane. In our experiments, the mitochondrial precursor-related proteins Atp5b and mt-Atp8 were reduced by HFD, but HFX reversed this effect. In addition, we provided evidence that mitochondrial biogenesis is increased in the HFX group.



**Fig 5. Protein-protein interaction scheme generated from differentially regulated protein upon HFD, and exercise focused on metabolism using STRING (version 11.0).**

<https://doi.org/10.1371/journal.pone.0273049.g005>

The essential proteins that control mitochondrial biogenesis, such as cytochrome b-c1 complex subunit 2, isovaleryl-CoA dehydrogenase, and hydroxymethylglutaryl-CoA synthase, were all upregulated in the liver of the HFX mice, compared with the HFD mice. Some previous studies have suggested that exercise improves the function of mitochondrial biogenesis even though the mice were fed an HFD. Lezi et al. observed that 6 weeks of moderate-intensity treadmill exercise increased mitochondrial biogenesis [48]. Gehrke et al. demonstrated that VWR increased mitochondrial fatty acid  $\beta$ -oxidation in the liver of mice fed a HFD for 12 weeks [49]. These findings suggested that HFD decreases energy metabolism and the expression of mitochondrial precursor-related proteins, but exercise reverses these effects in the liver.

Specifically, several essential pathways, including those related to the metabolism of xenobiotics and lipids, were downregulated, resulting in a decrease in SBP2 and Phyh (*LN1*) protein levels in HFD-fed mice. SBP2 is expressed in the liver and has specific properties of binding with xenobiotics like selenium and acetaminophen [50, 51]. Zhou et al. demonstrated that the high fat- and fast food-fed mice groups showed downregulated pathways of carbohydrate/lipid metabolism, including the downregulated expression of *Selenbp2*, but exercise could alleviate the altered DNA methylation induced by the high-fat or fast-food diet [52]. In addition, our experimental results showed that SBP2 levels were increased in HFX mice, corroborating the findings of previous studies. However, the exact role of SBP2 in liver pathology is unclear, but

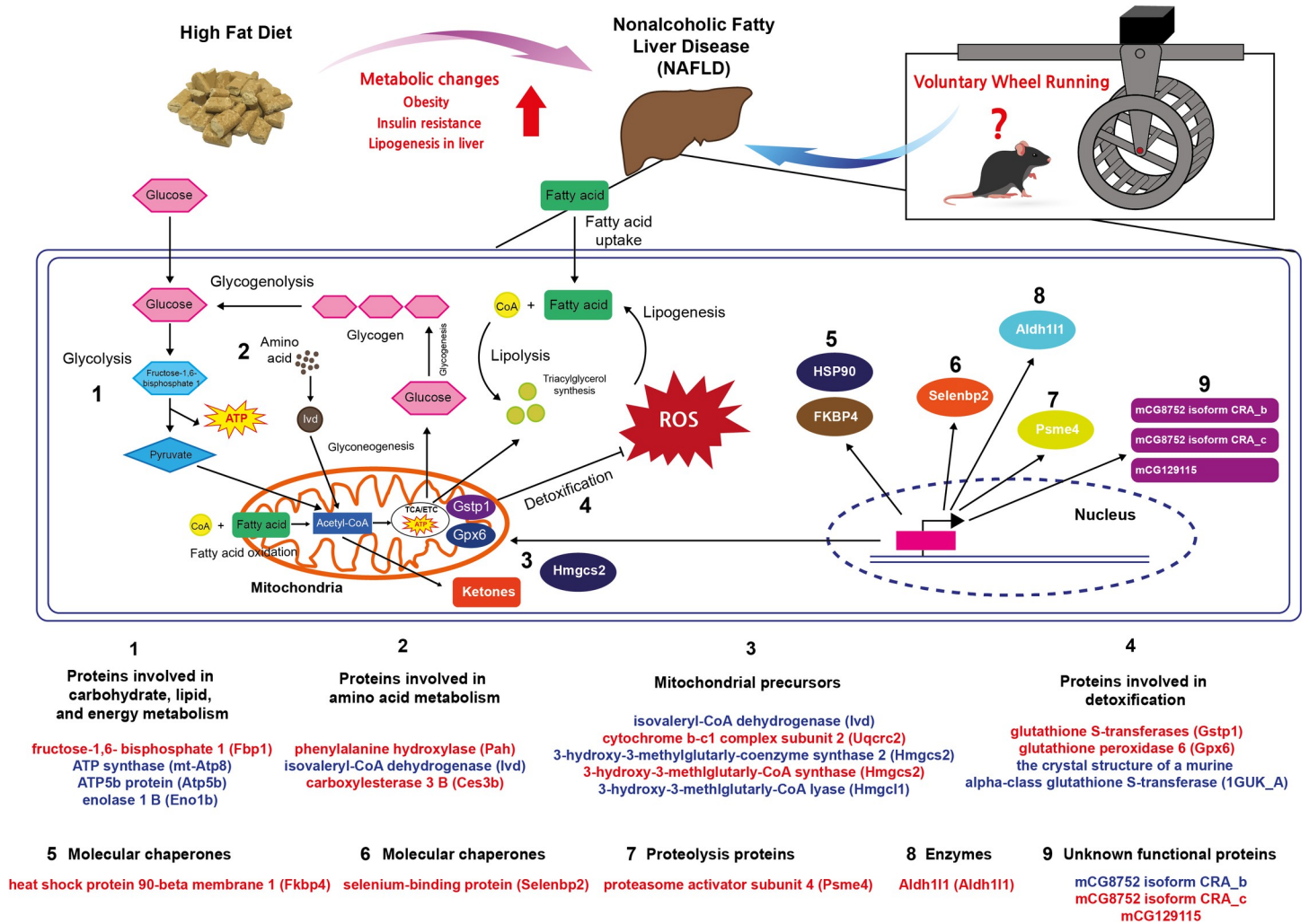


**Fig 6. Summary of differentially expressed liver proteins from a high-fat diet and 12 weeks of voluntary wheel running intervention.** Interpretation of proteomic analysis results by LC-MS/MS based on enriched functional annotation of proteins present at higher or lower levels in HFX compared to HFD. Proteins were grouped according to their functional properties into nine categories, as shown in the figure. ATP, adenosine triphosphate; TCA, tricarboxylic acid cycle; ETC, electron transport chain; ROS, reactive oxygen species; CoA, coenzyme A. Red color denotes upregulated protein expression in the HFX group compared to the HFD group and blue color indicates downregulated protein expression in the HFD group compared to the CON group.

<https://doi.org/10.1371/journal.pone.0273049.g006>

its alteration in response to exercise can make it a novel therapeutic target in various liver diseases. Exercise improves lipid metabolism in the liver. Phyh (LN1) is known to convert phytanoyl-CoA to 2-hydroxyphytanoyl-CoA, which is a process of lipid metabolism, and activate  $\beta$ -oxidation [53]. Our study indicated that 12 weeks of VWR increased the expression of the lipid metabolism-related proteins Fbp1, Atp5b, and mt-Atp8.

Aerobic organisms inevitably produce reactive oxygen species (ROS), which are byproducts of oxidative metabolism that could induce oxidative damage to cells [54]. In general, a cell has antioxidant enzymes that protect against the detrimental effects of ROS [54]. However, disrupting the ROS-antioxidant balance under physiological conditions leads to excessive ROS production and the prevalence of metabolic diseases [55]. Our results showed that exercise increased the expression of the liver antioxidant enzymes and proteolysis proteins. Glutathione S-transferase (GST) is a glutathione sulfur transferase enzyme essential for metabolizing pro-oxidant xenobiotics in the liver [54]. There is some evidence that endurance exercise can

upregulate liver GST levels, but HFD can downregulate its expression in the liver. Our data showed an increased expression of liver GST P1, 1GUK\_A, and Ceb3b after 12 weeks of VWR, suggesting that regular exercise, even with HFD, can increase the levels of antioxidant enzymes in the liver. Regular exercise may protect against excessive alterations in metabolism-related proteins and mitochondrial oxidative proteins.

In summary, in this study we were able to (1) screen the expression profiles of specific proteins in the liver by using MS/MS, (2) verify the functional role of these proteins in our experimental setup, and (3) understand the beneficial effects of exercise in specific pathophysiological conditions. The establishment of high fat diet-induced obesity mouse model is more challenging as a metabolic disease model than the genetic model of obesity, but it may closely resemble the environmental effects of human obesity. Various metabolic conditions, such as metabolic syndrome and NAFLD, can be confirmed by the protein spectrum associated with the disease, as implied by this study. Further understanding of the expression of proteins, such as changes in *de novo* protein synthesis in the liver through exercise, is needed to identify specific protein isoforms to understand mitochondrial bioenergetics under different conditions. The function of unknown proteins (e.g., MCG8752 and MCG129115) found in the current study can be explored in the context of NAFLD and exercise. The limitation of this study was that VWR assumed considerable changes in the expression of proteins, but we did not know the intensity and volume of exercise affecting protein expression in the liver. In addition, if the blood analysis, such as glucose, triglycerides, AST, and so on, was presented together with the current results, it would have supported the results.

In conclusion, in the present study we demonstrated that high-fat diet and regular exercise can modulate proteomics in the liver. The beneficial effects of voluntary wheel running in HFD-fed mice were reflected by the upregulation of gluconeogenesis, detoxification, mitochondrial biogenesis, and proteolysis pathways in the liver.

## Supporting information

**S1 Fig. Distribution of weekly running distance of mouse in HFX group.** In the middle of the box, the cross (+) indicates mean data.  
(TIF)

## Author Contributions

**Conceptualization:** Byunghun So, Li Li Ji, Chounghun Kang.

**Data curation:** Byunghun So, Li Li Ji, Chounghun Kang.

**Funding acquisition:** Chounghun Kang.

**Investigation:** Byunghun So, Chounghun Kang.

**Methodology:** Chounghun Kang.

**Project administration:** Chounghun Kang.

**Supervision:** Chounghun Kang.

**Validation:** Byunghun So, Li Li Ji, Saba Imdad, Chounghun Kang.

**Visualization:** Byunghun So, Chounghun Kang.

**Writing – original draft:** Byunghun So.

**Writing – review & editing:** Byunghun So, Li Li Ji, Saba Imdad, Chounghun Kang.

## References

1. Angulo P. Nonalcoholic fatty liver disease. *N Engl J Med*. 2002; 346:1221–1231. <https://doi.org/10.1056/NEJMra011775> PMID: 11961152
2. Takahashi Y, Soejima Y, Fukusato T. Animal models of nonalcoholic fatty liver disease/nonalcoholic steatohepatitis. *World J Gastroenterol*. 2012; 18:2300–2308. <https://doi.org/10.3748/wjg.v18.i19.2300> PMID: 22654421
3. Anstee QM, Reeves HL, Kotsiliti E, Govaere O, Heikenwalder M. From NASH to HCC: current concepts and future challenges. *Nat Rev Gastroenterol Hepatol*. 2019; 16:411–428. <https://doi.org/10.1038/s41575-019-0145-7> PMID: 31028350
4. Burt AD, Lackner C, Tiniakos DG. Diagnosis and Assessment of NAFLD: Definitions and Histopathological Classification. *Semin Liver Dis*. 2015; 35:207–220. <https://doi.org/10.1055/s-0035-1562942> PMID: 26378639
5. Flier JS. Obesity wars: molecular progress confronts an expanding epidemic. *Cell*. 2004; 116:337–350. [https://doi.org/10.1016/s0092-8674\(03\)01081-x](https://doi.org/10.1016/s0092-8674(03)01081-x) PMID: 14744442
6. You T, Yang R, Lyles MF, Gong D, Nicklas BJ. Abdominal adipose tissue cytokine gene expression: relationship to obesity and metabolic risk factors. *Am J Physiol Endocrinol Metab*. 2005; 288:E741–747. <https://doi.org/10.1152/ajpendo.00419.2004> PMID: 15562250
7. Vernon G, Baranova A, Younossi ZM. Systematic review: the epidemiology and natural history of non-alcoholic fatty liver disease and non-alcoholic steatohepatitis in adults. *Aliment Pharmacol Ther*. 2011; 34:274–285. <https://doi.org/10.1111/j.1365-2036.2011.04724.x> PMID: 21623852
8. Buettner R, Scholmerich J, Bollheimer LC. High-fat diets: modeling the metabolic disorders of human obesity in rodents. *Obesity (Silver Spring)*. 2007; 15:798–808. <https://doi.org/10.1038/oby.2007.608> PMID: 17426312
9. EASL-EASD-EASO Clinical Practice Guidelines for the management of non-alcoholic fatty liver disease. *J Hepatol*. 2016; 64:1388–1402. <https://doi.org/10.1016/j.jhep.2015.11.004> PMID: 27062661
10. Chalasani N, Younossi Z, Lavine JE, Charlton M, Cusi K, Rinella M, et al. The diagnosis and management of nonalcoholic fatty liver disease: Practice guidance from the American Association for the Study of Liver Diseases. *Hepatology*. 2018; 67:328–357. <https://doi.org/10.1002/hep.29367> PMID: 28714183
11. Febbraio MA. Exercise metabolism in 2016: Health benefits of exercise—more than meets the eye! *Nat Rev Endocrinol*. 2017; 13:72–74. <https://doi.org/10.1038/nrendo.2016.218> PMID: 28051119
12. Kim YJ, Kim HJ, Lee WJ, Seong JK. A comparison of the metabolic effects of treadmill and wheel running exercise in mouse model. *Lab Anim Res*. 2020; 36:3. <https://doi.org/10.1186/s42826-019-0035-8> PMID: 32206610
13. Greenwood BN, Fleshner M. Voluntary Wheel Running: A Useful Rodent Model for Investigating the Mechanisms of Stress Robustness and Neural Circuits of Exercise Motivation. *Curr Opin Behav Sci*. 2019; 28:78–84. <https://doi.org/10.1016/j.cobeha.2019.02.001> PMID: 32766411
14. Kawanishi N, Niihara H, Mizokami T, Yada K, Suzuki K. Exercise training attenuates neutrophil infiltration and elastase expression in adipose tissue of high-fat-diet-induced obese mice. *Physiol Rep*. 2015;3. <https://doi.org/10.14814/phy2.12534> PMID: 26341995
15. Kawanishi N, Yano H, Mizokami T, Takahashi M, Oyanagi E, Suzuki K. Exercise training attenuates hepatic inflammation, fibrosis and macrophage infiltration during diet induced-obesity in mice. *Brain Behav Immun*. 2012; 26:931–941. <https://doi.org/10.1016/j.bbi.2012.04.006> PMID: 22554494
16. Goncalves IO, Passos E, Rocha-Rodrigues S, Diogo CV, Torrella JR, Rizo D, et al. Physical exercise prevents and mitigates non-alcoholic steatohepatitis-induced liver mitochondrial structural and bioenergetics impairments. *Mitochondrion*. 2014; 15:40–51. <https://doi.org/10.1016/j.mito.2014.03.012> PMID: 24727595
17. Bradley RL, Jeon JY, Liu FF, Maratos-Flier E. Voluntary exercise improves insulin sensitivity and adipose tissue inflammation in diet-induced obese mice. *Am J Physiol Endocrinol Metab*. 2008; 295:E586–594. <https://doi.org/10.1152/ajpendo.00309.2007> PMID: 18577694
18. Evans CC, LePard KJ, Kwak JW, Stancukas MC, Laskowski S, Dougherty J, et al. Exercise prevents weight gain and alters the gut microbiota in a mouse model of high fat diet-induced obesity. *PLoS One*. 2014; 9:e92193. <https://doi.org/10.1371/journal.pone.0092193> PMID: 24670791
19. Kasch J, Schumann S, Schreiber S, Klaus S, Kanzleiter I. Beneficial effects of exercise on offspring obesity and insulin resistance are reduced by maternal high-fat diet. *PLoS One*. 2017; 12:e0173076. <https://doi.org/10.1371/journal.pone.0173076> PMID: 28235071
20. Ghareghani P, Shanaki M, Ahmadi S, Khoshdel AR, Rezvan N, Meshkani R, et al. Aerobic endurance training improves nonalcoholic fatty liver disease (NAFLD) features via miR-33 dependent autophagy induction in high fat diet fed mice. *Obes Res Clin Pract*. 2018; 12:80–89. <https://doi.org/10.1016/j.orcp.2017.01.004> PMID: 28163011

21. Baranova A, Liotta L, Petricoin E, Younossi ZM. The role of genomics and proteomics: technologies in studying non-alcoholic fatty liver disease. *Clin Liver Dis*. 2007; 11:209–220, xi. <https://doi.org/10.1016/j.cld.2007.02.003> PMID: 17544980
22. Tyers M, Mann M. From genomics to proteomics. *Nature*. 2003; 422:193–197. <https://doi.org/10.1038/nature01510> PMID: 12634792
23. Wilkins MR, Pasquali C, Appel RD, Ou K, Golaz O, Sanchez JC, et al. From proteins to proteomes: large scale protein identification by two-dimensional electrophoresis and amino acid analysis. *Biotechnology (N Y)*. 1996; 14:61–65. <https://doi.org/10.1038/nbt0196-61> PMID: 9636313
24. Yamaguchi W, Fujimoto E, Higuchi M, Tabata I. A DIGE proteomic analysis for high-intensity exercise-trained rat skeletal muscle. *J Biochem*. 2010; 148:327–333. <https://doi.org/10.1093/jb/mvq073> PMID: 20634418
25. Deshmukh AS. Proteomics of Skeletal Muscle: Focus on Insulin Resistance and Exercise Biology. *Proteomes*. 2016;4. <https://doi.org/10.3390/proteomes4010006> PMID: 28248217
26. National Research Council Committee for the Update of the Guide for the Care and Use of Laboratory Animals. The National Academies Collection: Reports funded by National Institutes of Health. *Guide for the Care and Use of Laboratory Animals*. Washington (DC): National Academies Press (US) Copyright © 2011, National Academy of Sciences.; 2011.
27. Cho YM, Bae SH, Choi BK, Cho SY, Song CW, Yoo JK, et al. Differential expression of the liver proteome in senescence accelerated mice. *Proteomics*. 2003; 3:1883–1894. <https://doi.org/10.1002/pmic.200300562> PMID: 14625850
28. Choi BK, Chitwood DJ, Paik YK. Proteomic changes during disturbance of cholesterol metabolism by azacoprostane treatment in *Caenorhabditis elegans*. *Mol Cell Proteomics*. 2003; 2:1086–1095. <https://doi.org/10.1074/mcp.M300036-MCP200> PMID: 12904448
29. Hardy T, Oakley F, Anstee QM, Day CP. Nonalcoholic Fatty Liver Disease: Pathogenesis and Disease Spectrum. *Annu Rev Pathol*. 2016; 11:451–496. <https://doi.org/10.1146/annurev-pathol-012615-044224> PMID: 26980160
30. Abenavoli L, Milic N, Di Renzo L, Preveden T, Medić-Stojanoska M, De Lorenzo A. Metabolic aspects of adult patients with nonalcoholic fatty liver disease. *World J Gastroenterol*. 2016; 22:7006–7016. <https://doi.org/10.3748/wjg.v22.i31.7006> PMID: 27610012
31. Byrne CD, Targher G. NAFLD: a multisystem disease. *J Hepatol*. 2015; 62:S47–64. <https://doi.org/10.1016/j.jhep.2014.12.012> PMID: 25920090
32. Than NN, Newsome PN. A concise review of non-alcoholic fatty liver disease. *Atherosclerosis*. 2015; 239:192–202. <https://doi.org/10.1016/j.atherosclerosis.2015.01.001> PMID: 25617860
33. Farzanegi P, Dana A, Ebrahimipour Z, Asadi M, Azarbayjani MA. Mechanisms of beneficial effects of exercise training on non-alcoholic fatty liver disease (NAFLD): Roles of oxidative stress and inflammation. *Eur J Sport Sci*. 2019; 19:994–1003. <https://doi.org/10.1080/17461391.2019.1571114> PMID: 30732555
34. Zou Y, Qi Z. Understanding the Role of Exercise in Nonalcoholic Fatty Liver Disease: ERS-Linked Molecular Pathways. *Mediators Inflamm*. 2020; 2020:6412916. <https://doi.org/10.1155/2020/6412916> PMID: 32774148
35. Cordeira J, Monahan D. Voluntary wheel running reduces weight gain in mice by decreasing high-fat food consumption. *Physiol Behav*. 2019; 207:1–6. <https://doi.org/10.1016/j.physbeh.2019.04.019> PMID: 31028763
36. Capello M, Ferri-Borgogno S, Cappello P, Novelli F.  $\alpha$ -Enolase: a promising therapeutic and diagnostic tumor target. *Febs j*. 2011; 278:1064–1074. <https://doi.org/10.1111/j.1742-4658.2011.08025.x> PMID: 21261815
37. Gitlits VM, Toh BH, SENTRY JW. Disease association, origin, and clinical relevance of autoantibodies to the glycolytic enzyme enolase. *J Investig Med*. 2001; 49:138–145. <https://doi.org/10.2310/6650.2001.34040> PMID: 11288754
38. Guo Q, Wang Y, Xu D, Nossent J, Pavlos NJ, Xu J. Rheumatoid arthritis: pathological mechanisms and modern pharmacologic therapies. *Bone Res*. 2018; 6:15. <https://doi.org/10.1038/s41413-018-0016-9> PMID: 29736302
39. Subramanian A, Miller DM. Structural analysis of alpha-enolase. Mapping the functional domains involved in down-regulation of the c-myc protooncogene. *J Biol Chem*. 2000; 275:5958–5965. <https://doi.org/10.1074/jbc.275.8.5958> PMID: 10681589
40. Petrak J, Ivanek R, Toman O, Cmejla R, Cmejlova J, Vyoral D, et al. Déjà vu in proteomics. A hit parade of repeatedly identified differentially expressed proteins. *Proteomics*. 2008; 8:1744–1749. <https://doi.org/10.1002/pmic.200700919> PMID: 18442176



41. Lu D, Xia Q, Yang Z, Gao S, Sun S, Luo X, et al. ENO3 promoted the progression of NASH by negatively regulating ferroptosis via elevation of GPX4 expression and lipid accumulation. *Ann Transl Med.* 2021; 9:661. <https://doi.org/10.21037/atm-21-471> PMID: 33987359
42. de Wilde J, Mohren R, van den Berg S, Boekschoten M, Dijk KW, de Groot P, et al. Short-term high fat-feeding results in morphological and metabolic adaptations in the skeletal muscle of C57BL/6J mice. *Physiol Genomics.* 2008; 32:360–369. <https://doi.org/10.1152/physiolgenomics.00219.2007> PMID: 18042831
43. Wiśniewski JR, Friedrich A, Keller T, Mann M, Koepsell H. The impact of high-fat diet on metabolism and immune defense in small intestine mucosa. *J Proteome Res.* 2015; 14:353–365. <https://doi.org/10.1021/pr500833v> PMID: 25285821
44. Lamont BJ, Visinoni S, Fam BC, Kebede M, Weinrich B, Papapostolou S, et al. Expression of human fructose-1,6-bisphosphatase in the liver of transgenic mice results in increased glycerol gluconeogenesis. *Endocrinology.* 2006; 147:2764–2772. <https://doi.org/10.1210/en.2005-1498> PMID: 16497803
45. Jurica MS, Mesecar A, Heath PJ, Shi W, Nowak T, Stoddard BL. The allosteric regulation of pyruvate kinase by fructose-1,6-bisphosphate. *Structure.* 1998; 6:195–210. [https://doi.org/10.1016/s0969-2126\(98\)00021-5](https://doi.org/10.1016/s0969-2126(98)00021-5) PMID: 9519410
46. Trefts E, Williams AS, Wasserman DH. Exercise and the Regulation of Hepatic Metabolism. *Prog Mol Biol Transl Sci.* 2015; 135:203–225. <https://doi.org/10.1016/bs.pmbts.2015.07.010> PMID: 26477916
47. Wasserman DH. Four grams of glucose. *Am J Physiol Endocrinol Metab.* 2009; 296:E11–21. <https://doi.org/10.1152/ajpendo.90563.2008> PMID: 18840763
48. E L, Lu J, Burns JM, Swerdlow RH. Effect of exercise on mouse liver and brain bioenergetic infrastructures. *Exp Physiol.* 2013; 98:207–219. <https://doi.org/10.1113/expphysiol.2012.066688> PMID: 22613742
49. Gehrke N, Biedenbach J, Huber Y, Straub BK, Galle PR, Simon P, et al. Voluntary exercise in mice fed an obesogenic diet alters the hepatic immune phenotype and improves metabolic parameters—an animal model of life style intervention in NAFLD. 2019; 9:4007. <https://doi.org/10.1038/s41598-018-38321-9> PMID: 30850619
50. Kirpich IA, Gobejishvili LN, Bon Homme M, Waigel S, Cave M, Arteel G, et al. Integrated hepatic transcriptome and proteome analysis of mice with high-fat diet-induced nonalcoholic fatty liver disease. *J Nutr Biochem.* 2011; 22:38–45. <https://doi.org/10.1016/j.jnutbio.2009.11.009> PMID: 20303728
51. Mattow J, Demuth I, Haeselbarth G, Jungblut PR, Klose J. Selenium-binding protein 2, the major hepatic target for acetaminophen, shows sex differences in protein abundance. *Electrophoresis.* 2006; 27:1683–1691. <https://doi.org/10.1002/elps.200500703> PMID: 16532517
52. Zhou D, Hlady RA, Schafer MJ, White TA, Liu C, Choi JH, et al. High fat diet and exercise lead to a disrupted and pathogenic DNA methylome in mouse liver. *Epigenetics.* 2017; 12:55–69. <https://doi.org/10.1080/15592294.2016.1261239> PMID: 27858497
53. Mukherji M, Kershaw NJ, Schofield CJ, Wierzbicki AS, Lloyd MD. Utilization of sterol carrier protein-2 by phytanoyl-CoA 2-hydroxylase in the peroxisomal alpha oxidation of phytanic acid. *Chem Biol.* 2002; 9:597–605. [https://doi.org/10.1016/s1074-5521\(02\)00139-4](https://doi.org/10.1016/s1074-5521(02)00139-4) PMID: 12031666
54. Ji LL, Leichtweis S. Exercise and oxidative stress: Sources of free radicals and their impact on antioxidant systems. *Age (Omaha).* 1997; 20:91–106. <https://doi.org/10.1007/s11357-997-0009-x> PMID: 23604295
55. Peake JM, Markworth JF, Nosaka K, Raastad T, Wadley GD, Coffey VG. Modulating exercise-induced hormesis: Does less equal more? *J Appl Physiol (1985).* 2015; 119:172–189. <https://doi.org/10.1152/jappphysiol.01055.2014> PMID: 25977451